


**Magnetic field induced reconstruction of electronic structure in  $\text{Sr}_3\text{Ru}_2\text{O}_7$  nanosheets**Weiwei Chu,<sup>1,2</sup> Ning Wang,<sup>1</sup> Yan Liu,<sup>1,3</sup> Yu Wang,<sup>4</sup> Guoqiang Liu,<sup>5</sup> Yuyan Han,<sup>1</sup> Ning Hao,<sup>1</sup> Zhe Qu,<sup>1</sup> Jiyong Yang,<sup>1,6,\*</sup> Fei Xue,<sup>1,8</sup> Zhiqiang Mao,<sup>4</sup> and Mingliang Tian<sup>1,7,8,†</sup><sup>1</sup>Anhui Province Key Laboratory of Condensed Matter Physics at Extreme Conditions, High Magnetic Field Laboratory, Chinese Academy of Sciences, Hefei 230031, Anhui, China<sup>2</sup>Department of Physics, University of Science and Technology of China, Hefei 230031, Anhui, China<sup>3</sup>College of Physics and Electronic Engineering, Sichuan Normal University, Chengdu 610068, China<sup>4</sup>Department of Physics, Pennsylvania State University, University Park, Pennsylvania 16802, USA<sup>5</sup>Ningbo Institute of Material Technology and Engineering, Chinese Academy of Sciences, Ningbo 315201, China<sup>6</sup>School of Physical Science and Technology, Southwest University, Chongqing 400715, China<sup>7</sup>School of Physics and Materials Science, Anhui University, Hefei 230601, Anhui, China<sup>8</sup>Collaborative Innovation Center of Advanced Microstructures, Nanjing University, Nanjing 210093, China (Received 7 February 2020; revised 16 September 2020; accepted 29 October 2020; published 12 November 2020)

The origin of the large magnetoresistance (MR) peak induced by the metamagnetic transition (MMT) in  $\text{Sr}_3\text{Ru}_2\text{O}_7$  has attracted extensive attention, but still remains puzzling. Here we performed systematic magnetotransport and torque magnetometry measurements of  $\text{Sr}_3\text{Ru}_2\text{O}_7$  nanosheets, and found surprisingly that the MR peak, together with the MMT, shifts dramatically toward low magnetic field with the decrease of thickness. Meanwhile, the Hall coefficient shows clearly a sign change near the MR peak position, indicating a magnetic field induced change of band topology. Combined with the theoretical calculation, we argue that the nature of the MR peak in  $\text{Sr}_3\text{Ru}_2\text{O}_7$  is associated with the so-called Lifshitz transition due to van Hove singularity, which is closer to the Fermi level in thinner nanosheets.

DOI: [10.1103/PhysRevB.102.195119](https://doi.org/10.1103/PhysRevB.102.195119)

$\text{Sr}_3\text{Ru}_2\text{O}_7$  belongs to the perovskite ruthenates of the Ruddlesden-Popper series  $\text{Sr}_{n+1}\text{Ru}_n\text{O}_{3n+1}$  ( $n = 1, 2, \infty$ ) with  $n = 2$  [1]. Contrasted with the  $n = 1$  member  $\text{Sr}_2\text{RuO}_4$ , which is an unconventional superconductor [2–4],  $\text{Sr}_3\text{Ru}_2\text{O}_7$  is a paramagnetic metal in its ground state [5], and shows two unusual metamagnetic transitions (MMTs), manifested by a superlinear increase in magnetization at critical magnetic fields of  $\sim 8$  T and 13.5 T for  $H \parallel c$  (or  $\sim 5.5$  T and 5.8 T for  $H \parallel ab$  plane) [6,7]. A very striking and puzzling phenomenon is that, accompanied by the first MMT, the magnetoresistance (MR) exhibits simultaneously a huge peak [6–8]. Although this phenomenon has been extensively studied for decades [6,8–11], its nature remains controversial.

One theoretical work based on the phenomenological Ginzburg-Landau theory suggests that the MR peak at the first MMT may be caused by the magnetic Condon domain wall scattering of electrons [12], but a subsequent experimental study suggests it may originate from the magnetic field induced electronic nematic order (ENO) [10,13–15], which is manifested by the formation of a spin density wave (SDW) [11]. Thus, the MR peak is reasonably attributed to the gapping out of Fermi surface or the SDW domain wall scattering

of electrons [11]. However, the entropy and specific heat experiments [16–18] show that there are still large number of carriers at the MR peak position, suggesting the former might be ruled out. Unfortunately, the domain scenario is also challenged by a recent domain tuning experiment [19], in which no hysteresis in the MR curves is observed by repeatedly driving the magnetic field passing over or across the critical field at the MR peak.

Previously, few were known when the thickness of  $\text{Sr}_3\text{Ru}_2\text{O}_7$  is in the nanometer scale. A recent transport experiment on the 20 nm-thick  $\text{Sr}_3\text{Ru}_2\text{O}_7$  thin film shows that the electron nematic phase can be promoted to much higher temperatures and over a larger magnetic field range than in bulk single crystals, which is attributed to the strain effect arising from the lattice mismatch between the film and substrate [20]. In this work, we focus on the MR behavior of single crystalline  $\text{Sr}_3\text{Ru}_2\text{O}_7$  nanosheets, which are freestanding on the Si/SiO<sub>2</sub> substrate. We found the MR peak shifts considerably toward low magnetic fields with the decrease of nanosheet thickness. Hall effect and magnetic property measurements reveal that there is a magnetic field induced sign change of the Hall coefficient at the MR peak position, suggesting a possible Lifshitz transition. Theoretical calculation shows that the above results can be understood by the van Hove singularity, which is closer to the Fermi level in thinner nanosheets.

The preparation of nanosheets for experimental measurements is presented in the Supplemental Material [21]. Figure 1 shows the resistance ( $R$ ) versus temperature ( $T$ ) curve of a  $\text{Sr}_3\text{Ru}_2\text{O}_7$  nanosheet with a thickness  $d$  of 30 nm, where the

\*To whom correspondence should be addressed: [jyyang@swu.edu.cn](mailto:jyyang@swu.edu.cn)†To whom correspondence should be addressed: [tianml@hmfll.ac.cn](mailto:tianml@hmfll.ac.cn)

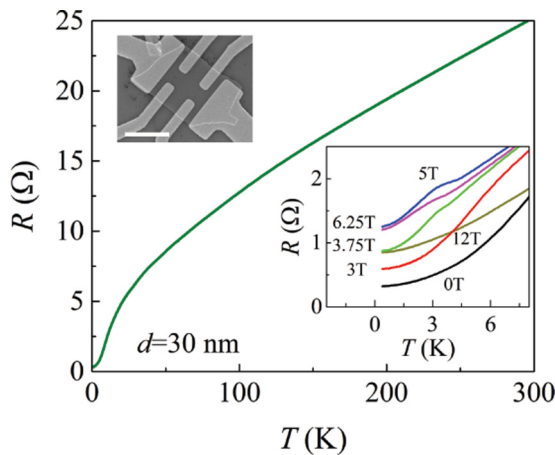


FIG. 1. Temperature ( $T$ ) dependent resistance ( $R$ ) of a 30 nm-thick  $\text{Sr}_3\text{Ru}_2\text{O}_7$  nanosheet. Insets: (Top) A scanning electronic microscopy image of the nanosheet. Scale bar:  $3 \mu\text{m}$ . (Bottom) Magnetic field dependence of the  $R$ - $T$  behavior of the 30 nm-thick nanosheet.

top inset shows a scanning electronic microscopy image of the nanosheet. It is found that the  $R$  decreases monotonically with decreasing  $T$ , with a residual resistance ratio ( $RRR$ ) of about 80, which is in line with those reported in bulk  $\text{Sr}_3\text{Ru}_2\text{O}_7$  single crystals [5,9]. The enlargement of the  $R$ - $T$  curves at different magnetic fields is shown in the bottom inset, a kink at  $\sim 4.0$  K emerges clearly when the magnetic field  $H$  is near 5.0 T. A similar  $H$ -dependent  $R$ - $T$  property showing kinks at  $\sim 4.0$  K is also observed in 200 nm-thick nanosheet [21]. It has been reported that a  $H$ -dependent kink in the  $R$ - $T$  curve can be observed only below  $\sim 1.0$  K in ultrapure single crystalline  $\text{Sr}_3\text{Ru}_2\text{O}_7$  bulk [22] due to the formation of magnetic field induced ENO or SDW [10,11,13]. Our results indicate that the characteristic temperature showing the unusual kinks in nanosheets is much higher than  $\sim 1.0$  K due to the thickness confinement effect. All nanosheets used in this work exhibit very similar  $R$ - $T$  dependence, indicating our samples do not involve intergrowth with either  $\text{Sr}_4\text{Ru}_3\text{O}_{10}$  or  $\text{SrRuO}_3$  [23].

Figure 2 shows  $R$ - $H$  curves of nanosheets with various thickness measured at 0.5 K with  $H\parallel c$ . No hysteresis is observed in the MR when sweeping the magnetic field back and forth, which is consistent with previous reports of bulk samples [6,8]. A significant feature is that the peak position ( $H_p$ ) of the MR shifts dramatically toward the low field with decreasing the thickness. The detailed definition of  $H_p$  is presented in Fig. S3 [21]. For comparison, the  $R$ - $H$  curve of a  $\text{Sr}_3\text{Ru}_2\text{O}_7$  bulk single crystal measured with  $H\parallel c$  is plotted in the inset of Fig. 2(a), where the  $H_p$  is  $\sim 7.9$  T.

It is well known that the MR peak for a bulk sample takes place at the MMT, with a critical field identical to  $H_p$ . However, for a nanosheet, it is unclear whether its MMT also follows the similar thickness dependence of the MR. In general, it is very challenging to obtain the magnetization data on a nanosheet due to its extreme small magnetic moments. Here, we performed torque magnetometry measurements on  $\text{Sr}_3\text{Ru}_2\text{O}_7$  nanosheets using an ultrasensitive cantilever with low spring constant ( $\sim 10$  mN/m) [24,25]. With this technique, a single piece of the  $\text{Sr}_3\text{Ru}_2\text{O}_7$  nanosheet was attached

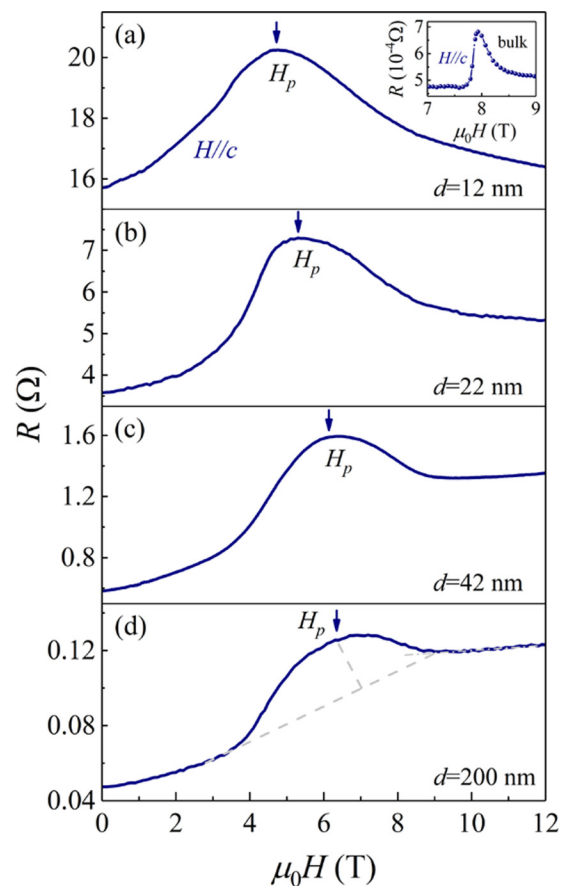


FIG. 2. Magnetic field dependent resistance for different-thickness  $\text{Sr}_3\text{Ru}_2\text{O}_7$  nanosheets measured at 0.5 K with  $H\parallel c$ . (a)  $d = 12$  nm; (b)  $d = 22$  nm; (c)  $d = 42$  nm; (d)  $d = 200$  nm. Inset in (a):  $R$ - $H$  curve of a  $\text{Sr}_3\text{Ru}_2\text{O}_7$  bulk single crystal with  $H\parallel c$  at 0.5 K.

to the free end of the Si cantilever, as shown in Fig. 3(a). When a magnetic field is applied, the magnetic torque  $\tau = M \times H$  ( $M$ : magnetization) would induce a displacement  $\Delta x$  of the cantilever, which is in proportion to  $\tau$ .

Figures 3(b) and 3(c) show, respectively, the  $H$ -dependent  $\tau$  of 800 nm- and 200 nm-thick nanosheets measured at 2.2 K and 1.6 K, where  $\theta$  is the angle between the  $H$  and the  $ab$  plane of the nanosheet, as schematically shown in the inset of Fig. 3(b). Two successive transitions at critical fields of  $H_{c1}$  and  $H_{c2}$ , which must correspond to the first and second MMTs, can be identified from the  $d\tau/dH$ - $H$  plot, as representatively shown in the inset of Fig. 3(c) [7]. The angle  $\theta$ -dependent  $H_{c1}$  and  $H_{c2}$  of the two samples are summarized in Figs. 3(d) and 3(e), respectively. It is found that both  $H_{c1}$  and  $H_{c2}$  decrease with decreasing  $\theta$ , which is consistent with previous magnetic torque measurements of a bulk sample [7]. The facts that both  $H_{c1}$  and  $H_{c2}$  are reduced significantly with decreasing thickness for  $H\parallel c$  compared with the bulk ( $H_{c1} \sim 8$  T,  $H_{c2} \sim 13.5$  T [7]), and the magnitude of  $H_{c1}$  is almost identical to  $H_p$  in the 200 nm-thick nanosheet, suggest the MMTs and the MR peak indeed share a same thickness-dependent behavior as expected.

To understand the origin of the MR peak at the MMT, we performed systematic Hall resistivity measurements at

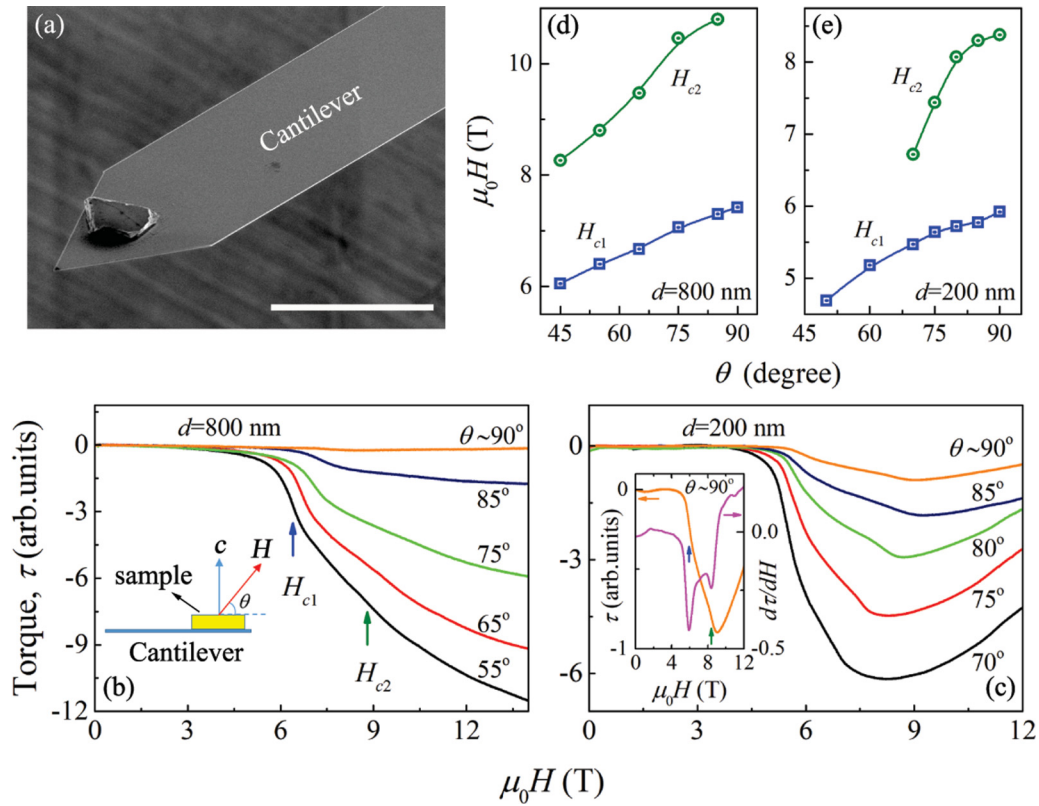


FIG. 3. (a) A scanning electronic microscopy image of the 800 nm-thick  $\text{Sr}_3\text{Ru}_2\text{O}_7$  nanosheet attached at the free end of an Si cantilever for the torque magnetometry measurement. Scale bar: 100  $\mu\text{m}$ . (b) and (c) are, respectively, the magnetic field dependent torque as a function of the angle  $\theta$  defined in the inset of (b) of the 800 nm-thick nanosheet measured at  $T = 2.2$  K and the 200 nm-thick nanosheet measured at  $T = 1.6$  K. Inset of (c) is an enlarged view of the magnetic field dependent torque (left axis) and its corresponding derivative (right axis) measured near  $\theta \sim 90^\circ$  of the 200 nm-thick nanosheet, where the first and second magnetic transition critical fields  $H_{c1}$  and  $H_{c2}$  are, respectively, defined at the minimum of the  $d\tau/dM$ - $H$  curve. (d) and (e) are, respectively, the angle-dependent critical fields of the 800 nm and 200 nm-thick nanosheets.

0.5 K on several nanosheets as shown in Fig. 4(a), where  $\rho_{xy} = [\rho_{xy}(H) - \rho_{xy}(-H)]/2$  is obtained by symmetrizing the data with positive and negative field cycles. One can find that  $\rho_{xy}$  increases linearly with increasing  $H$  up to a magnetic field of  $H_1$ , then changes its slope from positive to negative with three distinguishable kinks at  $H_1$ ,  $H_2$ , and  $H_3$ , respectively, as labeled by the arrows. Note that the kinks above  $H_1$  are not distinguishable in the  $\text{Sr}_3\text{Ru}_2\text{O}_7$  bulk reported in Ref. [26]. The critical fields at the kinks are summarized in Fig. 4(b) as a function of nanosheet thickness,  $d$ . It is clearly seen that  $H_3$  is almost thickness independent for  $d < 200$  nm, and remains at  $\sim 10$  T. However,  $H_1$  and  $H_2$  decrease with decreasing thickness, which almost follow the same thickness-dependent behavior of the MR peak and the MMT [see Fig. 4(b) and Fig. S4 [21],  $H_1$ : “ $\Delta$ ”,  $H_p$ : “ $\star$ ”,  $H_{c1}$ : “ $\square$ ”,  $H_2$ : “ $\circ$ ”,  $H_{c2}$ : “ $\diamond$ ”. These results indicate that the kinks at  $H_1$  and  $H_2$  in  $\rho_{xy}$  must correspond to  $H_{c1}$  (or  $H_p$  of the MR) and  $H_{c2}$  of the MMT.  $H_3$  can thus reasonably be considered as a characteristic field of the magnetic field induced high moment phase [11].

As a metamagnetic metal of  $\text{Sr}_3\text{Ru}_2\text{O}_7$ , its total Hall resistivity,  $\rho_{xy}$ , should involve both ordinary Hall effect (OHE) and anomalous Hall effect (AHE) with  $\rho_{xy} = R_H^{\text{OHE}}H + R_H^{\text{AHE}}M$  [27], where  $M$  is the magnetization along the  $c$  axis,  $R_H^{\text{OHE}}$  and  $R_H^{\text{AHE}}$  are, respectively, the ordinary and anomalous Hall coefficients. However, combined with the

magnetic measurements, we conclude that the AHE has less contribution to  $\rho_{xy}$ . This is based on the observation that in the MMT range of  $H_1 < H < H_3$ , as shown in Fig. S1 [21] and Ref. [6,11], the change of magnetization is  $\sim 0.1\mu_B/Ru$  per Tesla, which is about five times larger than that outside of this region, but the variation of  $\rho_{xy}$  at  $H_1 < H < H_3$  is not so significant compared with that at  $H < H_1$  and  $H > H_3$ , which is completely contrary to the AHE theory [27]. Since the traces of the  $\rho_{xy}$ - $H$  curves for nanosheets of different thicknesses, as shown in Fig. 4(a), are almost parallel to each other at low fields ( $< H_1$ ), suggesting the transport property of the nanosheet is less dependent on the thickness below  $H_1$ . The low field ( $< H_1$ ) Hall coefficient  $R_H$ , extracted from the slope of the  $\rho_{xy}$ - $H$  curves, is about  $2 \times 10^{-10} \text{ m}^3/\text{C}$  [Fig. 4(c)], which is consistent with that determined from bulk samples [28,29]. Strikingly, a clear sign change of  $R_H$  from positive at  $H < H_1$  to negative at  $H > H_3$  in each  $\text{Sr}_3\text{Ru}_2\text{O}_7$  nanosheet is observed [Fig. 4(c)], indicating there possibly exists a magnetic field induced band structure reconstruction [21]. One possibility is the so-called Lifshitz (LF) transition where the Fermi surface topology changes due to the variations of the Fermi energy and/or the band structure [30]. Such a LF transition effectively modifies the transport properties, hence the MR peaks at the transition field. The fact that above  $H_3$ ,  $R_H$  decreases with decreasing thickness [Fig. 4(c)], indicates that

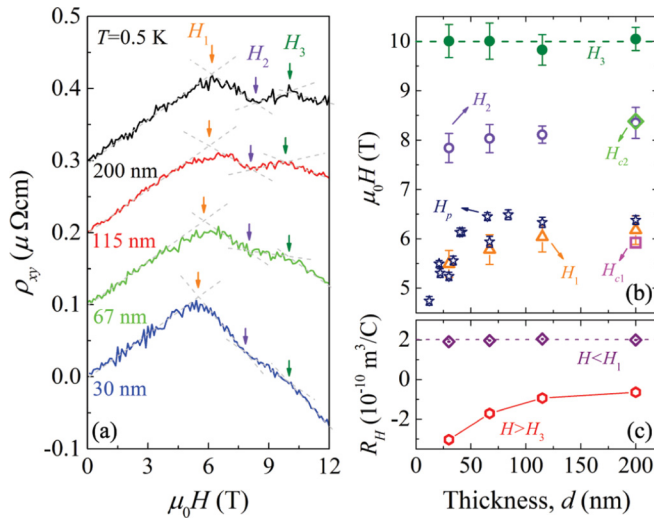


FIG. 4. (a) Magnetic field dependent Hall resistivity  $\rho_{xy}$  of  $\text{Sr}_3\text{Ru}_2\text{O}_7$  nanosheets with different thicknesses  $d$  measured at 0.5 K. The kinks of the  $\rho_{xy}$ - $H$  slope changes are labeled as  $H_1$ ,  $H_2$ ,  $H_3$ , respectively. Curves are shifted vertically by  $0.1 \mu\Omega\text{cm}$  for clarity. (b) Magnetic field  $H$  versus nanosheet thickness  $d$ . The characteristic fields,  $H_p$ ,  $H_1$ ,  $H_2$ ,  $H_3$ , and the critical fields of  $H_{c1}$  and  $H_{c2}$ , are labeled by symbols “ $\star$ ”, “ $\Delta$ ”, “ $\circ$ ”, “ $\bullet$ ”, “ $\square$ ”, “ $\diamond$ ” respectively. (c) Thickness dependence of the Hall coefficient  $R_H$  at  $H < H_1$  and  $H > H_3$ .

the MMT and the accompanied MR peak are indeed sensitive to the band structure or the position of the Fermi level ( $E_F$ ).

LF transition can be induced by chemical doping or pressure through continuously tuning the filling of a band or the shape of a Fermi surface, as already argued in cuprates [31], iron pnictides [32], and topological materials [33], etc. LF transition can also be driven by a magnetic field through coupling with the Zeeman term, but it is usually achieved in heavy fermion system when the Fermi energy is significantly reduced due to the hybridization of the conduction and the localized  $f$  electrons [34,35]. The observation of magnetic field induced LF transition under low magnetic fields ( $H_1 \sim 6$  T) in  $\text{Sr}_3\text{Ru}_2\text{O}_7$  is extremely striking, since its Zeeman energy is small [36]. However, our observation seems to be a reminiscent of recent theoretical studies [37–41], showing the MMT in  $\text{Sr}_3\text{Ru}_2\text{O}_7$  is related to a van Hove singularity in the density of state (DOS). In this scenario, the band feature is considered to be very sensitive to small energy scales and the Zeeman energy tends to reconstruct the Fermi surface via strong spin orbital coupling and/or quenching of orbital moments rather than just causing a relative chemical potential shift [13,37–40].

To get an insight into the thickness-dependent  $H_p$  (or  $H_1$ ), density functional theory (DFT) calculations are performed [21]. It was known that the structure relaxation for a  $\text{Sr}_3\text{Ru}_2\text{O}_7$  sheet including only two  $\text{Sr}_3\text{Ru}_2\text{O}_7$  units along the  $c$  direction causes a slight expansion of the lattice constant  $c$  to be 2.085 nm through a total energy minimization, compared to 2.059 nm for a bulk structure, indicating the  $c$  more likely increases with the decrease of nanosheet thickness (this is qualitatively consistent with our experimental observation [21]). Similar lattice change is reported in thin

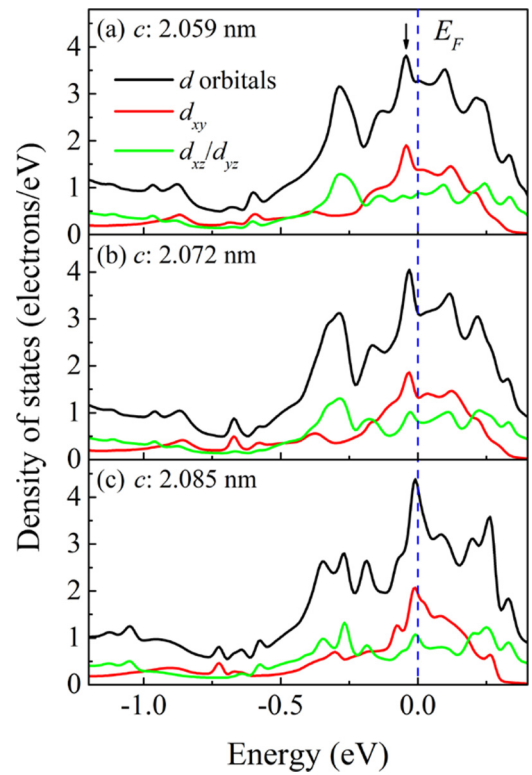


FIG. 5. Partial density of states for the Ru  $d$  orbitals with (a)  $c = 2.059$  nm, (b)  $c = 2.072$  nm, and (c)  $c = 2.085$  nm. The arrow in (a) denotes a van Hove singularity.

transition-metal dichalcogenides [42]. Figure 5 presents the partial density of state (PDOS) of Ru with different lattice constant  $c$ ; the total DOS is shown in the Supplemental Material [21]. A sharp peak near the  $E_F$  of the PDOS referred to a van Hove singularity, which is marked by the arrow in Fig. 5(a) can be found, consistent with previous theoretical calculation [38]. Interestingly, we found the van Hove singularity shifts toward the  $E_F$  as  $c$  increases. Since the position of the van Hove singularity is mainly determined by the  $d_{xy}$  orbital of Ru (Fig. 5), such a shift can thus be attributed to the change of crystal field. When  $c$  increases, the elongated  $\text{RuO}_6$  octahedra causes the  $d_{xy}$  orbital to be upward shifted relative to the  $d_{xz}/d_{yz}$  orbitals. In  $\text{Ca}_2\text{RuO}_4$  and  $\text{Ca}_3\text{Ru}_2\text{O}_7$ , it has been reported that the flattening of  $\text{RuO}_6$  octahedra causes the downward shift of the  $d_{xy}$  orbital, leading to an orbital polarization [43,44]. Considering the van Hove singularity is responsible for the MMT (e.g., Ref. [41]) and the sign change of  $R_H$  shown in Fig. 4(c), the thickness-tuned shift of the van Hove singularity towards the  $E_F$  might be the origin of the thickness-dependent MR peak or the MMT as well as the magnetic field induced LF transition.

In summary, we have systematically studied the thickness dependence of magnetotransport and magnetic properties of  $\text{Sr}_3\text{Ru}_2\text{O}_7$  single crystalline nanosheets. We found that the first MMT as well as its resulting MR peak shift to low magnetic field with decreasing thickness. Combined with the Hall resistivity and torque magnetometry measurements, and the DFT calculation, we argue that the anomalous MR peak at the MMT might originate from a magnetic field induced LF transition due to van Hove singularity.

This work was supported by the National Natural Science Foundation of China (Grants No. U19A2093, No. 11674323, No. 11804297, No. 11774352, No. 11774305, No. U1432251, and No. U1832214); Collaboration Innovation Program of Hefei Science Center, CAS (Grant No. 2019HSC-CIP 001);

the CAS/SAFEA international partnership program for creative research teams of China. The work at PSU is supported by the US National Science Foundation under Grant No. DMR 1917579.

- [1] H. Shaked, J. D. Jorgensen, O. Chmaissem, S. Ikeda, and Y. Maeno, *J. Solid State Chem.* **154**, 361 (2000).
- [2] K. Ishida, H. Mukuda, Y. Kitaoka, K. Asayama, Z. Q. Mao, Y. Mori, and Y. Maeno, *Nature (London)* **396**, 658 (1998).
- [3] C. W. Hicks, D. O. Brodsky, E. A. Yelland, A. S. Gibbs, J. A. N. Bruin, M. E. Barber, S. D. Edkins, K. Nishimura, S. Yonezawa, Y. Maeno, and A. P. Mackenzie, *Science* **344**, 283 (2014).
- [4] A. Steppke, L. Zhao, M. E. Barber, T. Scaffidi, F. Jerzembeck, H. Rosner, A. S. Gibbs, Y. Maeno, S. H. Simon, A. P. Mackenzie, and C. W. Hicks, *Science* **355**, eaaf9398 (2017).
- [5] S.-I. Ikeda, Y. Maeno, S. Nakatsuji, M. Kosaka, and Y. Uwatoko, *Phys. Rev. B* **62**, R6089 (2000).
- [6] R. S. Perry, L. M. Galvin, S. A. Grigera, L. Capogna, A. J. Schofield, A. P. Mackenzie, M. Chiao, S. R. Julian, S. I. Ikeda, S. Nakatsuji, Y. Maeno, and C. Pfleiderer, *Phys. Rev. Lett.* **86**, 2661 (2001).
- [7] E. Ohmichi, Y. Yoshida, S. I. Ikeda, N. V. Mushnikov, T. Goto, and T. Osada, *Phys. Rev. B* **67**, 024432 (2003).
- [8] S. A. Grigera, P. Gegenwart, R. A. Borzi, F. Weickert, A. J. Schofield, R. S. Perry, T. Tayama, T. Sakakibara, Y. Maeno, A. G. Green, and A. P. Mackenzie, *Science* **306**, 1154 (2004).
- [9] S. A. Grigera, R. S. Perry, A. J. Schofield, M. Chiao, S. R. Julian, G. G. Lonzarich, S. I. Ikeda, Y. Maeno, A. J. Millis, and A. P. Mackenzie, *Science* **294**, 329 (2001).
- [10] R. A. Borzi, S. A. Grigera, J. Farrell, R. S. Perry, S. J. S. Lister, S. L. Lee, D. A. Tennant, Y. Maeno, and A. P. Mackenzie, *Science* **315**, 214 (2007).
- [11] C. Lester, S. Ramos, R. S. Perry, T. P. Croft, R. I. Bewley, T. Guidi, P. Manuel, D. D. Khalyavin, E. M. Forgan, and S. M. Hayden, *Nature Mater.* **14**, 373 (2015).
- [12] B. Binz, H. B. Braun, T. M. Rice, and M. Sigrist, *Phys. Rev. Lett.* **96**, 196406 (2006).
- [13] S. Raghu, A. Paramekanti, E. A. Kim, R. A. Borzi, S. A. Grigera, A. P. Mackenzie, and S. A. Kivelson, *Phys. Rev. B* **79**, 214402 (2009).
- [14] H. Doh, Y. B. Kim, and K. H. Ahn, *Phys. Rev. Lett.* **98**, 126407 (2007).
- [15] C. Stingl, R. S. Perry, Y. Maeno, and P. Gegenwart, *Phys. Rev. Lett.* **107**, 026404 (2011).
- [16] A. W. Rost, R. S. Perry, J.-F. Mercure, A. P. Mackenzie, and S. A. Grigera, *Science* **325**, 1360 (2009).
- [17] A. W. Rost, S. A. Grigera, J. A. N. Bruin, R. S. Perry, D. Tian, S. Raghu, S. A. Kivelson, and A. P. Mackenzie, *Proc. Natl. Acad. Sci.* **108**, 16549 (2011).
- [18] Y. Tokiwa, M. Mchawat, R. S. Perry, and P. Gegenwart, *Phys. Rev. Lett.* **116**, 226402 (2016).
- [19] D. O. Brodsky, M. E. Barber, J. A. N. Bruin, R. A. Borzi, S. A. Grigera, R. S. Perry, A. P. Mackenzie, and C. W. Hicks, *Sci. Adv.* **3**, e1501804 (2017).
- [20] P. B. Marshall, K. Ahadi, H. Kim, and S. Stemmer, *Phys. Rev. B* **97**, 155160 (2018).
- [21] See Supplemental Material at <http://link.aps.org/supplemental/10.1103/PhysRevB.102.195119> for details of (i) preparation of  $\text{Sr}_3\text{Ru}_2\text{O}_7$  nanosheets, (ii) magnetic field dependent  $R$ - $T$  data of the 200 nm-thick nanosheet, (iii) the extraction of  $H_p$ , (iv) thickness-dependent  $H_p$  of the MR,  $H_{c1}$  and  $H_{c2}$  of the MMT,  $H_1$ ,  $H_2$ , and  $H_3$  of the Hall resistivity in the thickness range of 0–800 nm, (v) analysis of the possible Lifshitz transition, (vi) calculation methods, (vii) total density of states of  $\text{Sr}_3\text{Ru}_2\text{O}_7$  with different lattice constant  $c$ , (viii) the lattice parameter  $c$  of a 30 nm-thick  $\text{Sr}_3\text{Ru}_2\text{O}_7$  nanosheet and the bulk single crystal. Includes additional references [1,6,7,28,45–50].
- [22] R. S. Perry, K. Kitagawa, S. A. Grigera, R. A. Borzi, A. P. Mackenzie, K. Ishida, and Y. Maeno, *Phys. Rev. Lett.* **92**, 166602 (2004).
- [23] Y. Liu, W. Chu, J. Yang, G. Liu, H. Du, W. Ning, L. Ling, W. Tong, Z. Qu, G. Cao, Z. Xu, and M. Tian, *Phys. Rev. B* **98**, 024425 (2018).
- [24] F. Xu, S. Guo, Y. Yu, N. Wang, L. Zou, B. Wang, R.-W. Li, and F. Xue, *Phys. Rev. Appl.* **11**, 054007 (2019).
- [25] A. Mehlin, F. Xue, D. Liang, H. F. Du, M. J. Stolt, S. Jin, M. L. Tian, and M. Poggio, *Nano Lett.* **15**, 4839 (2015).
- [26] R. A. Borzi, A. McCollam, J. A. N. Bruin, R. S. Perry, A. P. Mackenzie, and S. A. Grigera, *Phys. Rev. B* **84**, 205112 (2011).
- [27] N. Nagaosa, J. Sinova, S. Onoda, A. H. MacDonald, and N. P. Ong, *Rev. Mod. Phys.* **82**, 1539 (2010).
- [28] Y. Liu, R. Jin, Z. Q. Mao, K. D. Nelson, M. K. Haas, and R. J. Cava, *Phys. Rev. B* **63**, 174435 (2001).
- [29] R. S. Perry, L. M. Galvin, A. P. Mackenzie, D. M. Forsythe, S. R. Julian, S. I. Ikeda, and Y. Maeno, *Physica B* **284**, 1469 (2000).
- [30] I. M. Lifshitz, *Soviet Physics-JETP* **11**, 1130 (1960).
- [31] D. LeBoeuf, N. Doiron-Leyraud, B. Vignolle, M. Sutherland, B. J. Ramshaw, J. Levallois, R. Daou, F. Laliberté, O. Cyr-Choinière, J. Chang, Y. J. Jo, L. Balicas, R. Liang, D. A. Bonn, W. N. Hardy, C. Proust, and L. Taillefer, *Phys. Rev. B* **83**, 054506 (2011).
- [32] B. Lei, J. H. Cui, Z. J. Xiang, C. Shang, N. Z. Wang, G. J. Ye, X. G. Luo, T. Wu, Z. Sun, and X. H. Chen, *Phys. Rev. Lett.* **116**, 077002 (2016).
- [33] G. E. Volovik, *Low Temp. Phys.* **43**, 47 (2017).
- [34] G. Bastien, A. Gourgout, D. Aoki, A. Pourret, I. Sheikin, G. Seyfarth, J. Flouquet, and G. Knebel, *Phys. Rev. Lett.* **117**, 206401 (2016).
- [35] H. Pfau, R. Daou, S. Friedemann, S. Karbassi, S. Ghannadzadeh, R. Kuchler, S. Hamann, A. Steppke, D. Sun, M. König, A. P. Mackenzie, K. Kliemt, C. Krellner, and M. Brando, *Phys. Rev. Lett.* **119**, 126402 (2017).
- [36] K. Iwaya, S. Satow, T. Hanaguri, N. Shannon, Y. Yoshida, S. I. Ikeda, J. P. He, Y. Kaneko, Y. Tokura, T. Yamada, and H. Takagi, *Phys. Rev. Lett.* **99**, 057208 (2007).
- [37] M. H. Fischer and M. Sigrist, *Phys. Rev. B* **81**, 064435 (2010).

- [38] C. M. Puetter, J. G. Rau, and H.-Y. Kee, *Phys. Rev. B* **81**, 081105(R) (2010).
- [39] A. M. Berridge, *Phys. Rev. B* **83**, 235127 (2011).
- [40] W.-C. Lee and C. Wu, *Chin. Phys. Lett.* **33**, 037201 (2016).
- [41] M. Behrmann, C. Piefke, and F. Lechermann, *Phys. Rev. B* **86**, 045130 (2012).
- [42] W. S. Yun, S. W. Han, S. C. Hong, I. G. Kim, and J. D. Lee, *Phys. Rev. B* **85**, 033305 (2012).
- [43] J. H. Jung, Z. Fang, J. P. He, Y. Kaneko, Y. Okimoto, and Y. Tokura, *Phys. Rev. Lett.* **91**, 056403 (2003).
- [44] J. Peng, M. Q. Gu, X. M. Gu, G. T. Zhou, X. Y. Gao, J. Y. Liu, W. F. Xu, G. Q. Liu, X. Ke, L. Zhang, H. Han, Z. Qu, D. W. Fu, H. L. Cai, F. M. Zhang, Z. Q. Mao, and X. S. Wu, *Phys. Rev. B* **96**, 205105 (2017).
- [45] A. B. Pippard, *Magnetoresistance in Metal* (Cambridge University Press, Cambridge, 1989), p.253.
- [46] A. Tamai, M. P. Allan, J. F. Mercure, W. Meevasana, R. Dunkel, D. H. Lu, R. S. Perry, A. P. Mackenzie, D. J. Singh, Z.-X. Shen, and F. Baumberger, *Phys. Rev. Lett.* **101**, 026407 (2008).
- [47] N. P. Ong, *Phys. Rev. B* **43**, 193 (1991).
- [48] A. P. Mackenzie, N. E. Hussey, A. J. Diver, S. R. Julian, Y. Maeno, S. Nishizaki, and T. Fujita, *Phys. Rev. B* **54**, 7425 (1996).
- [49] G. Kresse and J. Furthmüller, *Phys. Rev. B* **54**, 11169 (1996).
- [50] P. Blaha *et al.*, computer code WIEN2K, (TU Wien, Vienna, 2001).